

COMBINATION OF MULTISENSOR 3D DATA WITH ERROR BOUNDS

G. Boström, J.G.M. Gonçalves, V. Sequeira

European Commission - Joint Research Centre, TP210, I-21020 Ispra, Italy

E-mail: vitor.sequeira@jrc.it

ABSTRACT

This paper address the steps associated to re-construct a model based on a number of scans acquired with different sensor techniques. It discusses the concept of managing and operating on scans with different origins, which may have different spatial resolution, accuracy and coverage. In order to cope with these varying sensor characteristics, it introduces the concept of error-bound to all points. This error-bound describes the uncertainty with which further operations on the point need to be considered. Furthermore, the paper discusses the concepts of modified registration and fusion/integration using the error-bound concept in order to achieve the best possible model based on the inserted scans. The technique described in the paper has been applied to a reconstruction project for parts of the city centre of Verona, Italy.

1. INTRODUCTION

To build realistic 3D models that match the physical world as accurately as possible, 3D reconstruction of very large outdoors environments is performed combining several kinds of data, such as: ground and aerial laser range scans, tracking data, ground, aerial and satellite images. Combining data from different sensors to form a solid reconstructed 3D Model is a difficult topic and the technique needs to cope with situations where the sensor data has various spatial resolutions, accuracy and noise. The data needs to be fused in a way where all data gives its best contribution to the final result.

Our previous work has been devoted to reconstruct large outdoor areas. For these purposes, we have designed and implemented a laser scanner mounted on a vehicle [1] enabling rapid model reconstruction of large urban areas.

This paper addresses the problems of making use of raw scan information from various sources having distinct differences in resolution and accuracy. We focus on the situations where the raw scan data to be used may have areas with significant errors. By constructing a toolbox of operations which correctly treats datasets having known errors distributions, we can more properly tackle the problems of treating information from virtually any sensor architecture provided that the built-in error bounds are known.

2. COMPLEXITY OF 3D DATA FUSION

2.1 Acquisition methods

Different techniques for acquiring 3D information exist. Each technique introduces inaccuracies specific to the acquisition methodology used.

Laser range scanners can operate accurately in the range from a couple of meters to above a kilometre. The accuracy and spatial resolution can be very good resulting in a very large amount of data observations of the target.

Aerial scans are normally acquired from airplanes with LIDAR or TLS-based systems technique. The information generally covers roof-tops and ground data with accuracy down to some centimetres.

Laser Range Finder transported by Vehicle has been introduced during the last years [1, 2, 3]. This type of device can quickly acquire the façade of houses in urban areas. This type of sensor-systems gives partly dense information and partly sparse information depending on the vehicle movement speed and turn. Also, the final accuracy can vary considerably as the trajectory is less accurate in certain areas during the scan.

There are other techniques such as depth from image sequences and other 3D scanning techniques. These techniques are not discussed further in this paper.

2.2 Error bound introduced

Each measurement performed can be associated with an error, ϵ . We use the term error-bound as the uncertainty for a given measurement. For a given 3D point, p , the error bound is the sphere with radius ϵ around p where the true position should be found, see Figure 1. For simplicity reasons, we assign a uniform probability distribution inside the sphere where to find the true value.

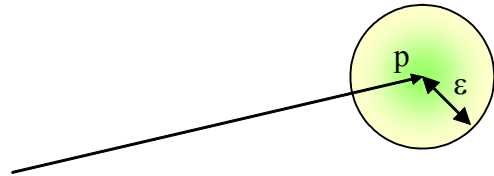


Figure 1. A measured 3D position with an assigned error-bound.

Below, the most important errors associated to range measurements are listed.

Range error:

A distance measurement itself is always affected by uncertainty, although the actual error can be considered as being very low in today's most advanced devices.

Alignment errors:

Apart from the actual range-uncertainty, the deviation of the measurement direction affects the final results. When considering the uncertainty of eventual mirror angles, encoders, vibrations and other effects, the error contributing to the total error can be significant.

The 3D from a vehicle mounted laser range scanner is highly being dependant on the reconstructed trajectory with which the vehicle was displaced. A small uncertainty in this path easily results in errors far bigger than all the other error-sources previously mentioned, Figure 2 and Figure 3.

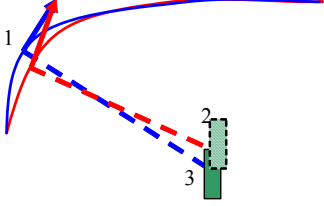


Figure 2: Effect of miscalculation of vehicle trajectory, 1, resulting in different re-calibrated object positions, 2, 3.

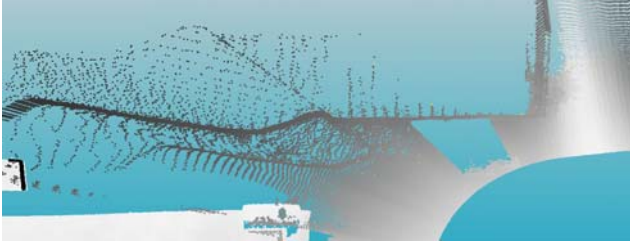


Figure 3: Sample of error in reconstructed wall due to error in trajectory reconstruction. Model has error-bound as colours (white: small error-bound, black: large error-bound)

Aerial Scan data:

For aerial data the uncertainty is difficult to calculate. For direct range measurements, we can find values from sensor data-sheets but the data undergoes several steps such as various mathematical filters and re-sampling. The result however, always gives a 3D data points with fairly big inaccuracy for our purposes. This means that we can assign a rather modest error for each point based on the sample distance.

Other error sources:

Other existing error sources which can be applied to points relate for example from registration errors.

Final treatment of errors:

Since all these error contributions can be considered as independent from each other we can for any given technology or cause sum the squared error from each contributing error.

$$\varepsilon_{tot} = \sqrt{\sum \varepsilon_i^2} \quad (\text{eq. 1})$$

2.3 Scanner techniques and error bound outlined

Here we will describe the error-equations which can be found for the different sensor techniques discussed in this paper.

Below, the following letters are used to denote measures:

d = range measurement, ε_d = range error, $\Delta\varphi$ = tilt uncertainty (rad), $\Delta\gamma$ = pan uncertainty (rad), $\Delta\theta$ = trajectory pan

uncertainty, ε_{reg} = registration error, ε_t = trajectory position error, Δg = grid-spacing, k = grid uncertainty factor.

Laser range finder mounted on a tripod:

The scanning technique uses deviation of the measurement beam in a pan and a tilt angle. The final error-equation can be written as:

$$\varepsilon_{tot} = \sqrt{\varepsilon_c^2 + \varepsilon_d^2 + (d\Delta\varphi)^2 + (d\Delta\gamma)^2 + \varepsilon_{reg}^2} \quad (\text{eq. 2})$$

Vehicle mounted laser range finder:

The error-bound for the points measurements heavily depend on the validity of the reconstructed trajectory. There are two sources of errors for a trajectory, ε_t , the trajectory uncertainty and $\Delta\theta$ the trajectory pan uncertainty. The final equation can be written as:

$$\varepsilon_{tot} = \sqrt{\varepsilon_t^2 + \varepsilon_c^2 + \varepsilon_d^2 + (d\Delta\varphi)^2 + (d\Delta\theta)^2 + \varepsilon_{reg}^2} \quad (\text{eq. 3})$$

Digital Surface Models:

The error-bound associated for the points coming from the resampled grid are assigned a value based on the grid spacing as:

$$\varepsilon_{tot} = \sqrt{\varepsilon_{reg}^2 + (k\Delta g)^2} \quad (\text{eq. 4})$$

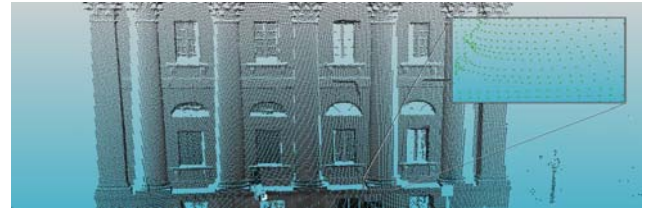


Figure 4: Error bound for a Laser Scan mounted on a tripod. The magnified part shows the pillar-base with a sub-sampling of 8 with visible error-bound.

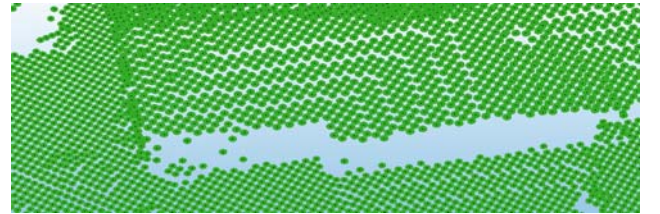


Figure 5: Error bound for part of a DSM. The entire image covers some 90x40 meters. The visible error-bounds all have 0.5 meter of radius.



Figure 6: Part of the vehicle board scan. The marked area shows visible error-bound for the lamp-post.

3. THE RECONSTRUCTION PARADIGM

3.1 Registration with Error-bounds

Since for each single measurement, we have an error-bound, we can introduce a weighting factor to the registration. Our proposal for the considerations of known error-bounds is to introduce a weighting ICP algorithm.

Two distinct modifications of the iterative ICP algorithm are introduced:

1. Modification of the selection of matching point-pairs by using modified Euclidian distance.
2. Modified solid-transform computation based on weighting among point-pairs.

Introduction of weight value:

In order to make use of the error-bound as an absolute weight we here introduce the weight function. The weight-function maps an error-bound ε , to a weight-value c . We have made use of the simplest, yet useful mapping that can be found:

$$c(w) = e^{(-2\varepsilon)} \quad (\text{eq. 5})$$

Selection of point-pairs:

An important aspect of the ICP algorithm which has been discussed extensively in the literature is how to best find matching points, i.e. for a given point in one scan find the best suited point in the other scan which shall be used for the computation of a transformation. See reference [4] for a list of available techniques. We use a modified closest distance approach. This may give rise to a number of invalid pairings but since we are interested in doing the registration on a continuously increasing number of reference point cloud-based scans we still stick to this method. The selection of corresponding point-pairs is performed in finding the point-pair which have the smallest modified distance, d' . The modified distance is taken as the Euclidian distance divided by the arithmetic average of the potential point-pair's weight values.

$$d' = \frac{2\|p - q\|}{c_p + c_q} \quad (\text{eq. 6})$$

Since the modified distance not only described the distance but also gives an indication of the error associated, we can make use of the maximum allowed distance to take away outliers.

The effect is 2-fold. In volumes having coverage from several scans, which have distinct differences in accuracy, the more precise points will be selected more frequently, i.e. a natural selection of the best available measurements is made. The other effect which can be identified is that areas having joint low accuracy get more frequently banned as outlier points.

Weighted solid transformation computation:

The solid transformation computation uses a weighting schema where point-pairs with less joint error are having more influence on the final transformation. We are making use of the solid-transformation computation defined in [5]. The unknown solid transform (R, T) to be found between two point-sets, p and q , with weights c_p and c_q respectively, which describes the best possible transformation for dataset q onto dataset p , can be obtained by minimizing the energy or error function described in equation 7. Function $w(p_i, c_{p_i}, q_i, c_{q_i})$ describes the joint weight for the given point-pair (p_i, q_i) .

$$e = \sum_i w(p_i, c_{p_i}, q_i, c_{q_i}) \|(p_i - Rq_i) - T\|^2 \quad (\text{eq. 7})$$

3.2 Integration of data having estimated error-bounds

The integration-step should identify the most suitable points for a final model, removing overlapping areas and invalid points. In a case where the error-bound is known, we can also define rules how the assignment of points shall be done. In this work we are not considering triangulated surfaces. The result is purely based on point-sets and the result is always a set of points describing the final integrated model. We do not average points from different scans (surfaces); instead we consider the point-set which minimizes the overall error.

To perform an integration which takes into account the error-bound, we divide the entire volume in an octree. We stop the subdivision at certain criteria:

- When the division has reached a level where the voxel-side reaches below a pre-defined value
- When a voxel only contains a single measurement

The selection of points and removal of points can be described as:

```
For each  $p_k, k$ 
  If there exist a  $(p_m, e_m), m \neq k$ , such that
     $\|p_k - p_m\| < e_k$ 
    and  $|e_k - e_m| > C$ 
    and  $e_m < e_k$ ,
  then
     $p_k$  can be removed.
```

The constant C is a value enabling values close to each other having a difference in error of less than C to still contribute to the final model.

4. EXPERIMENTS

4.1 Data set used

We have applied the concept of registration of scans and the fusion step under the influence of error-bounds to a data-set consisting of data coming from 3 different sensor architectures. For the detailed façade, 2 terrestrial scans were acquired with a Tripod mounted laser range finder. A scan was acquired with a Vehicle mounted laser-range finder and finally a DSM acquired from an airplane covering mostly ground and roof-tops was added. The set of scans range from detailed highly accurate measurement points to scans with partly good and partly bad data.

4.2 Error-bound computation

The errors associated to all scans were calculated as follows:

Laser range scanners:

Data was taken from scanner datasheets for range and deviation uncertainties resulting in an uncertainty in the range of about 5 to 25 millimetres see Figure 4.

Vehicle borne laser range scanner:

The uncertainty for the vehicle trajectory was assigned a position accuracy of 20 centimetres. In order to account for turns performed by the vehicle, an angular error corresponding to 1 second angular movement was introduced, thus affecting all data acquired during vehicle-turns. The resulting uncertainty ranged from about 30 to 80 centimetres. This effect can be seen in Figure 6 as visible error-bounds.

Aerial DSM:

For the aerial DSM having a grid-spacing, Δg , of 1 meter we assigned an uncertainty value, k , of 0.5, thus the error for each

point according to equation 4 should give an error in the range of 0.5 meters. This error is shown in Figure 5.

4.3 Registration and Integration steps

The registration of the terrestrial scans was performed using the weighted ICP algorithm. This created a scan group of 2 terrestrial scans having an excellent matching towards each other. The vehicle scan was then registered with the weighting version of ICP.

Since the DSM data is distributed mainly on the roof-tops and on the ground, there are very little overlapping data to perform an ICP-operation on. To tackle this problem we performed a 2D façade registration as described in [6].

The resulting registered scan group now contains dense data on the façades of the building with measurements coming from in total 4 different scans. A point-based model of all scans can be seen in Figure 7. Note the Scan identified with a red colour which comes from the vehicle Scan. This data partly overlaps the other scans but having a low accuracy, the overlapping data should not contribute to the final fused model.



Figure 7: Rendered Point-cloud of the 4 registered scans all having different colours.

We applied the integration as discussed in Section 3.2 on the point-set shown in Figure 7. In order to get a feasible resolution of the resulting model we used an octree-box size threshold of 10 centimetres, thus continuing the octree-division until the bounding-box had a longest side less than 10 centimetres.



Figure 8: Integrated data-set with original scan origin as colours.

5. RESULTS

The initial dataset having 3.7 million points resulted in a fused data-set of 300 thousand points, keeping the best possible points (see Figure 8). There is a small gap between the vehicle based scan (red) and the tripod based scan (dark blue). This is due to

the fact that the measurements coming from the less accurate vehicle scan are removed because of the integration error-sphere constrain. Also it can be noted that small parts of the vehicle based scan still remains on the right façade simply because the error values together with registration misalignment was too large.

6. CONCLUSIONS

We have introduced the concept of error-bound making it possible to reconstruct models or large areas from different types of sensors. The concept includes both scan-registration under consideration of weights and a fusion/integration preserving the best measurements for the final model. The concept has been shown on a part of the Verona City Centre, Italy, and using scan data from 3 different sensor architectures.

Current work includes applying deformable registration technique for the vehicle based scans to correct for abnormal trajectory errors.

7. ACKNOWLEDGMENT

We would like to thank the city of Verona and the University of Brescia, Italy, for the kind co-operation and support when performing the data acquisitions. Also, we would like to thank Compagnia Generale Ripresearee S.p.A, Parma, Italy for kindly providing us with DSM data over the Verona City Centre.

The work presented was developed within VISNET, a European Network of Excellence (<http://www.visnet-noe.org>), funded under the European Commission IST FP6 programme".

8. REFERENCES

- [1] Boström G., Fiocco M., Puig D., Rossini A. and Gonçalves J.G.M., Sequeira V., - "Acquisition, Modelling and Rendering of Very Large Urban Environments", in *Proc. 2nd Int. Symposium on 3D Data Processing Visualization & Transmission*, Thessaloniki, Greece, September, 2004
- [2] C. Früh and A. Zakhor, "An Automated Method for Large-Scale, Ground-Based City Model Acquisition", in *International Journal of Computer Vision*, vol. 60, p. 5-24, October 2004
- [3] H. Zhao and R. Shibasaki, "A Vehicle-Borne Urban 3-D Acquisition System Using Single-Row Laser Range Scanners", *IEEE Transactions on systems, man, and cybernetics*, August 2003
- [4] S. Rusinkiewicz and M. Levoy "Efficient Variants of the ICP Algorithm", *Third International Conference on 3D Digital Imaging and Modeling*, 2001
- [5] Horn, B.K.P., "Closed-Form Solution of Absolute Orientation using Unit Quaternions," *Journal of the Optical Society A*, Vol. 4, No. 4, pp. 629-642, April 1987
- [6] M. Fiocco, G. Boström, J.G.M. Gonçalves and V. Sequeira, "Multisensor fusion for Volumetric Reconstruction of Large Outdoor Areas", *Fifth International Conference on 3D Digital Imaging and Modeling*, Ottawa, Canada, 2005.